THE JOURNAL OF PROSTHETIC DENTISTRY

RESEARCH AND EDUCATION

Stepwise stress testing of different CAD-CAM lithium disilicate veneer application methods applied to lithium disilicate substructures

Jaren T. May, DDS, MSD,[a] Anelyse Arata, DDS, MS, PhD,[b] Norman B. Cook, DDS, MS,[c] Kim E. Diefenderfer, DMD, MS,[d] Nelson B. Lima, MS, PhD,[e] Alexandre L. S. Borges, DDS, MS, PhD,[f] and Sabrina Feitosa, DDS, MS, PhD[g]

ABSTRACT

Statement of problem. Whether a computer-aided design and computer-aided manufacture (CAD-CAM) fabricated high-translucency lithium disilicate veneer on a lithium disilicate substructure would increase the strength of the restoration compared with a traditional feldspathic porcelain veneer is unclear.

Purpose. The purpose of this in vitro study was to evaluate the effect of different lithium disilicate veneer application methods on a lithium disilicate substructure on their biaxial flexural stress (BFS).

Material and methods. Lithium disilicate disks were fabricated so that when combined with the veneering disks, they had a dimension of 12×1.2 mm. Experimental groups were as follows (n=15): resin-bonded lithium disilicate veneer, lithium disilicate veneer adhesively cemented to lithium disilicate; sintered lithium disilicate veneer, lithium disilicate veneer sintered to lithium disilicate; sintered feldspathic veneer, feldspathic porcelain applied to lithium disilicate; and monolithic lithium disilicate, the control group. Weibull distribution survival analysis was used to compare the differences in the resistance to fracture after fatigue. The total number of cycles was analyzed by using 1-way ANOVA (α=.05). A finite element analysis (FEA) was also performed. The maximum principal stress (MPS) was used as the failure criterion.

Results. The sintered feldspathic veneer group had significantly lower fatigue resistance than sintered lithium disilicate veneer or resin-bonded lithium disilicate veneer (P<.05). The resin-bonded lithium disilicate veneer group showed significantly more fractured fragments than the other groups. No statistical difference was observed in the number of cycles. The lithium disilicate veneered groups presented similar resistance to fatigue as the monolithic specimens of the same overall dimensions. Higher peaks of MPS were observed for groups monolithic lithium disilicate, sintered lithium disilicate veneer, and sintered feldspathic veneer than for resin-bonded lithium disilicate veneer.

Conclusions. Veneering a lithium disilicate substructure with a lithium disilicate veneer, bonded or sintered, increased resistance to fatigue compared with a feldspathic porcelain veneer. The lithium disilicate veneer groups had similar fatigue resistance to that of the monolithic group. (J Prosthet Dent 2022;128:794-802)

Lithium disilicate is a popular esthetic ceramic dental restorative material because of its high flexural strength (396 MPa) compared with fine particle feldspar ceramic (125 MPa).[1] The modulus of elasticity for lithium disilicate (95 GPa) is similar to that of enamel, and the linear coefficient of thermal expansion and fracture toughness values are similar to those of dentin.[2] The increased strength comes from the 70% crystalline lithium disilicate filler and because this material can be processed under pressure to create a more uniform crystalline structure with fewer defects.[3] Moreover, the lithium disilicate glass matrix can be acid-etched and silanized, achieving excellent chemical bond strength with a resin cement system.[4,5] In

Supported by a grant from Delta Dental (Dental Master's Thesis Award Program) and by Indiana University School of Dentistry.
[a]Graduate student, Department of Biomedical Sciences and Comprehensive Care, Indiana University School of Dentistry (IUSD), Indianapolis, Ind.
[b]Research collaborator-volunteer, Nuclear and Energy Research Institute, Department of Materials Science and Technology Center, Sao Paulo, Brazil.
[c]Clinical Associate Professor, Department of Cariology, Operative Dentistry, and Dental Public Health, Indiana University School of Dentistry (IUSD), Indianapolis, Ind.
[d]Clinical Associate Professor, Department of Cariology, Operative Dentistry, and Dental Public Health, Indiana University School of Dentistry (IUSD), Indianapolis, Ind.
[e]Research collaborator-volunteer, Nuclear and Energy Research Institute, Department of Materials Science and Technology Center, Sao Paulo, Brazil.
[f]Associate Professor, Department of Dental Materials and Prosthodontics, Sao Paulo State University, Institute of Science and Technology, UNESP, Sao Jose dos Campos, Brazil.
[g]Clinical Assistant Professor, Department of Biomedical Sciences and Comprehensive Care, Indiana University School of Dentistry (IUSD), Indianapolis, Ind.

Clinical Implications

Using lithium disilicate (either resin-bonded or sintered) as an esthetic veneer results in an increase in fracture resistance in comparison with using a feldspathic veneering material, providing fracture resistance similar to that of a monolithic restoration with the same dimensions.

addition, multiple shades and translucencies are available, offering a choice between a monolithic restoration or as a substructure veneered with feldspathic porcelain to optimize esthetics.[6]

Newer technology and material improvements have led to the possibility of using of a thin (0.4 to 0.5 mm) computer-aided design and computer-aided manufacture (CAD-CAM) lithium disilicate layer as a higher translucency veneer (IPS e.max CAD monolithic solutions chairside: instructions for use. product information; Ivoclar AG) adhered or sintered over a lower translucency lithium disilicate substructure. The resulting crown has a more realistic translucency and can be fabricated efficiently. The restoration may be less susceptible to chipping or fracture than the traditional feldspathic veneered lithium disilicate.[7] However, ceramic restorations are vulnerable to defects and microcracks that can develop during the processing steps; therefore, their resistance to fracture under load requires assessment.[8,9]

This in vitro study investigated the effect of different lithium disilicate veneer application methods on a lithium disilicate substructure on the biaxial flexural stress (BFS) of lithium disilicate veneered substructure restorations. The BFS test has the advantage of less sensitivity to edge flaws and defects,[8,10] leading to results considered more reliable. The null hypothesis was that adhering or sintering a thin laminate layer of lithium disilicate on a lithium disilicate substructure will not result in increased biaxial flexural strength in comparison with sintered feldspathic porcelain on lithium disilicate.

MATERIAL AND METHODS

The specimens were fabricated according to ISO/FDIS 6872:2014(E).[11] As seen in Figure 1, 32-mm lithium disilicate noncrystalized blocks (e.max CAD; Ivoclar AG) were machined into cylinders on a lathe to create uniform cylinders (Ø=12 mm) and sectioned by using a low-speed diamond saw (IsoMet 1000; Buehler). Finishing and polishing steps (DS-20; Leco) were performed under running water using #600-, #800-, and #1200-grit silicon carbide papers. For the 3 experimental groups (sintered lithium disilicate veneer, resin-bonded lithium disilicate veneer, and sintered feldspathic veneer), disks that modeled a crown structure were fabricated from lithium disilicate cylinders (Ø=12×32 mm) sectioned into disks, polished, and then crystalized in a furnace (Programat CS; Ivoclar AG) following the manufacturer's instructions. The thickness of each substructure specimen after polishing was 0.7 mm.

The control group consisted of monolithic lithium disilicate specimens with dimensions of 1.2 ±0.05 mm after polishing and crystalized following the manufacturer's instructions. For the sintered lithium disilicate veneer group, thin veneers (Ø=12×0.5 mm) of precrystalized 32-mm lithium disilicate were cut, polished, and crystalized by using the same protocol. A thin layer of connecting porcelain (Lot# W01285. IPS e.max CAD Crystall, Add-On Connect; Ivoclar AG) was placed on the thicker lithium disilicate specimen, and a thin lithium disilicate disk was positioned on top. An acetate film was placed above and below the specimens, and a 1.96-N load applied for 1 minute while vibrating. The specimens were fired according to the manufacturer's instructions. To account for the thickness of the connecting sintering porcelain, the specimens were repolished and returned to 1.2 mm, removing some of the 0.7-mm-thick substructure disk.

For the resin-bonded lithium disilicate veneer group, a thin lithium disilicate veneer (Ø=12×0.5 mm) was resin bonded to the surface of a lithium disilicate substructure (Ø=12×0.7 mm), creating an overall specimen thickness of 1.2 mm. The specimen bonding surface was prepared by using a self-etching primer (Lot# X46 577, Monobond Etch & Prime; Ivoclar AG) applied with a microbrush for 20 seconds, left for 40 seconds, and rinsed for 30 seconds followed by the resin cement application (Lot#X21 834, Multilink Automix; Ivoclar AG). The veneer was positioned onto the prepared surface of the substructure disk. A 1.96-N load was applied for uniform dispersion of forces. The specimens were light polymerized (BluePhase; Ivoclar AG) at 6 different locations for 20 seconds each. The specimens were stored in water for 24 hours before testing.

For the sintered feldspathic veneer group, feldspathic porcelain was sintered on the surface of 0.7-mm lithium disilicate specimens. The specimens were placed into a stainless-steel mold (Ø=12×1.3 mm), and a thin wash layer of feldspathic veneering ceramic (Lot# W89584, IPS e.max Ceram; Ivoclar AG) combined with a build-up liquid (IPS e.max Ceram build up liquid; Ivoclar AG) was placed onto the disk and vibrated to reduce air bubbles. Specimens were then vacuum-fired and cooled to room temperature. Two or 3 layers were placed and fired with the same protocol. To accommodate for shrinkage of the veneering porcelain, the specimen thickness was

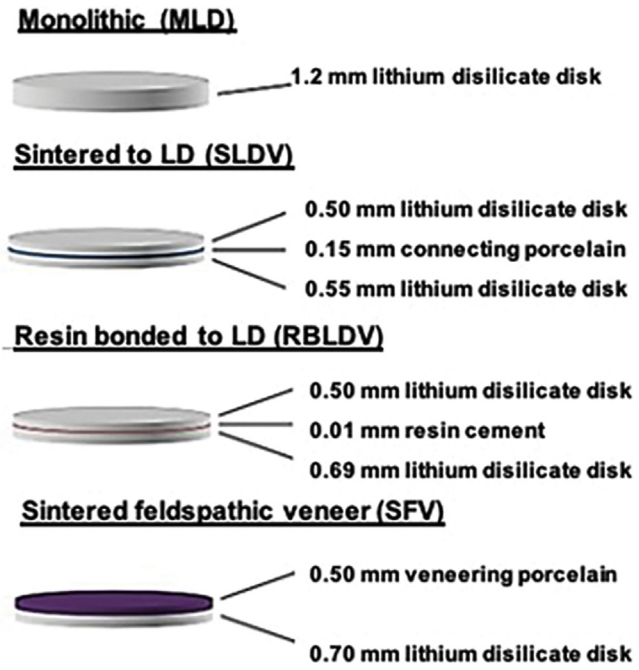

Figure 1. Experimental groups. MLD, monolithic lithium disilicate; RBLDV, resin-bonded lithium disilicate veneer; SLDV, sintered lithium disilicate veneer; SFV, sintered feldspathic veneer.

increased by 0.1 mm, and the feldspathic veneer side was then finished and polished to a 1.2-mm thickness.

Stepwise stress testing was performed by using a piston-on-ring configuration following ISO/FDIS 6872:2014(E). Specimens were tested up to 215 000 cycles at room temperature under dry conditions. The specimens were conditioned at 50 N for 5000 cycles and then increased by 50 N increments every 30 000 cycles with a load from 100 N up to 400 N. A frequency of 1.4 Hz on a universal testing machine (Electropuls E3000; Instron) was used with a crosshead speed of 0.5 mm per minute until fracture occurred. The load was applied from 3 hardened 4.5-mm-diameter steel balls placed 120 degrees apart on a support circle with a diameter of 11 mm. Load was applied with a flat piston with a diameter of 1.4 mm at the center of the specimen. To evenly distribute the forces, a 0.05-mm-thick acetate film was placed above and below the specimen.[8] Each specimen was evaluated for cracks or failures every 30 000 cycles under a light microscope.[12]

The Poisson ratios and Young modulus for the materials used are presented in Table 1.[13,14] The variation of the stresses through the thickness for the bilayer disks was calculated according to Equations 1 and 2 proposed by Hsueh et al in 2006[15] and varying the thickness from 0.1 mm to 1.2 mm.

Table 1. Material, Young modulus, Poisson ratio of materials used

Material	Young Modulus	Poisson Ratio	Reference
e.max CAD	95 GPa	0.20	13
Fusion Ceramic	70 GPa	0.21	13
Multilink	18.6 GPa	0.28	13
e.max Ceram	90 GPa	0.23	14
Stainless steel	200 GPa	0.30	Ansys library

$$\sigma_{r1}=\sigma_{\theta 1}=\frac{-PE_1(1+\nu)\left(Z-Z_n^*\right)}{8\pi\left(1-\nu_1^2\right)D^*}\times\left[1+2\ln\left(\frac{a}{c}\right)+\frac{1-\nu}{1+\nu}\left(1-\frac{c^2}{2a^2}\right)\frac{a^2}{R^2}\right] \quad (1)$$

(for $0\le Z\le t_1$ and $r\le c$),

$$\sigma_{r2}=\sigma_{\theta 2}=\frac{-PE_2(1+\nu)\left(Z-Z_n^*\right)}{8\pi\left(1-\nu_2^2\right)D^*}\times\left[1+2\ln\left(\frac{a}{c}\right)+\frac{1-\nu}{1+\nu}\left(1-\frac{c^2}{2a^2}\right)\frac{a^2}{R^2}\right] \quad (2)$$

(for $t_1\le Z\le t_1+t_2$ and $r=c$), where a, c, and R are the radii of the supporting ring, piston, and disk, respectively, and considering r the radial distance from the center of the disk and r, θ, and Z cylindrical coordinates. The neutral surface position and the flexural rigidity for all bilayer groups were obtained from Equations 3 and 4.

$$Z_n^*=\frac{\frac{E_1t_1^2}{2\left(1-\nu_1^2\right)}+\frac{E_2t_2^2}{2\left(1-\nu_2^2\right)}+\frac{E_2t_1t_2}{1-\nu}}{\frac{E_1t_1}{1-\nu_1^2}+\frac{E_2t_2}{1-\nu_2^2}} \quad (3)$$

$$D^*=\frac{E_1t_1^3}{3\left(1-\nu_1^2\right)}+\frac{E_2t_2^3}{3\left(1-\nu_2^2\right)}+\frac{E_2t_1t_2(t_1+t_2)}{1-\nu_2^2}-\frac{\left[\frac{E_1t_1^2}{2\left(1-\nu_1^2\right)}+\frac{E_2t_2^2}{2\left(1-\nu_2^2\right)}+\frac{E_2t_1t_2}{1-\nu_2^2}\right]^2}{\frac{E_1t_1}{1-\nu_1^2}+\frac{E_2t_2}{1-\nu_2^2}}, \quad (4)$$

where E is the Young modulus of each ceramic, and t_1 and t_2 are the overall thicknesses of each layer; the Poisson ratio of the bilayered disk is calculated by Equation 5.

$$\nu=\frac{\nu_1t_1+\nu_2t_2}{t_1+t_2}. \quad (5)$$

For the monolithic disks, the stress variation was calculated through Equations 6 and 7, where h_n is the total thickness of the specimen and ν is the Poisson ratio.[15]

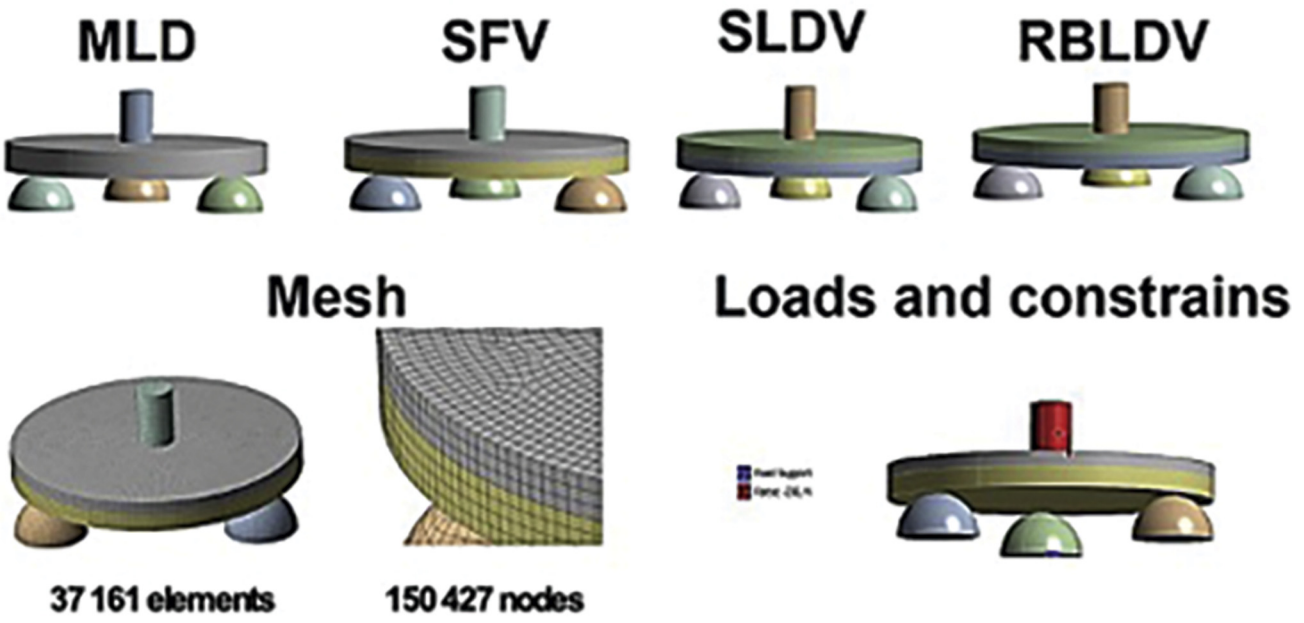

Figure 2. Three-dimensional model of experimental groups with mesh formed by tetrahedral elements. MLD, monolithic lithium disilicate; RBLDV, resin-bonded lithium disilicate veneer; SLDV, sintered lithium disilicate veneer; SFV, sintered feldspathic veneer.

Table 2. Load (N), number of fatigue cycles, number of pieces collected from the specimen after test, Weibull characteristic strength, Weibull modulus (m), peak of MPS

Group	N	Load (N)	N° Cycles	N° Pieces	Weibull Characteristic Strength[6]	Weibull Modulus (m)	Peak of MPS[6]
MLD	15	263 ±20	112 600 ±12 355	3.7 ±0.3[b]	289.7[ab]	4.6	179.78
SLDV	15	283 ±14	124 225 ±7952	3.5 ±0.3[b]	305.2[a]	5.6	180.55
RBLDV	15	293 ±13	124 455 ±8311	6.7 ±0.6[a]	314.5[a]	6.2	177.60
SFV	15	233 ±16	92 104 ±8903	3.5 ±0.2[b]	256.8[b]	4.1	182.78

MLD, monolithic lithium disilicate; MPS, maximum principal stress; RBLDV, resin-bonded lithium disilicate veneer; SFV, sintered feldspathic veneer; SLDV, sintered lithium disilicate veneer.

$$\sigma_r = \sigma_\theta = \frac{3P(1+\nu)}{4\pi h_n^3} \times \left[1 + 2\ln\left(\frac{a}{c}\right) + \frac{1-\nu}{1+\nu}\left(1 - \frac{c^2}{2a^2}\right)\frac{a^2}{R^2}\right] \quad (6)$$

(at z=0 and r≤c),

$$\sigma_r = \sigma_\theta = \frac{-3P(1+\nu)\left(z - \frac{h_n}{2}\right)}{2\pi h_n^3} \times \left[1 + 2\ln\left(\frac{a}{c}\right) + \frac{1-\nu}{1+\nu}\left(1 - \frac{c^2}{2a^2}\right)\frac{a^2}{R^2}\right] \quad (7)$$

(at r≤c).

Specimen fragments were submitted to scanning electron microscope (SEM, JSM-6390LV; JEOL) examination with a thin gold-palladium layer coated for 120 seconds by using a sputter coating machine (Desk V; Denton Vacuum). Digital images were submitted to qualitative evaluation. As seen in Figure 2, for the finite element analysis (FEA), a model was created for each experimental group in a CAD software program (Rhino 5.0; Rhinoceros) and exported to a computer-aided engineering (CAE) software (Products 2019 R1; ANSYS Inc), and a static structural analysis was performed. Hexahedrons (10 nodes) were used to mesh, and the quantity of elements was increased until 5% of convergence was achieved. All materials were considered homogeneous, linearly elastic, and isotropic; their properties are described in Table 1. Maximum principal stress (MPS) was used as the failure criteria.

The Weibull parametric survival analysis was used to compare biaxial flexural resistance to fracture among the 4 groups (α=.05). A Weibull distribution survival analysis compared the differences in resistance to fracture among the 4 groups. The resistance to fracture (N) was used as time to event for the analysis. The number of fragments into which the specimens fractured was analyzed by using a nonparametric test to compare the differences among the groups.

RESULTS

The Weibull distribution survival analysis showed that both the resin-bonded lithium disilicate veneer

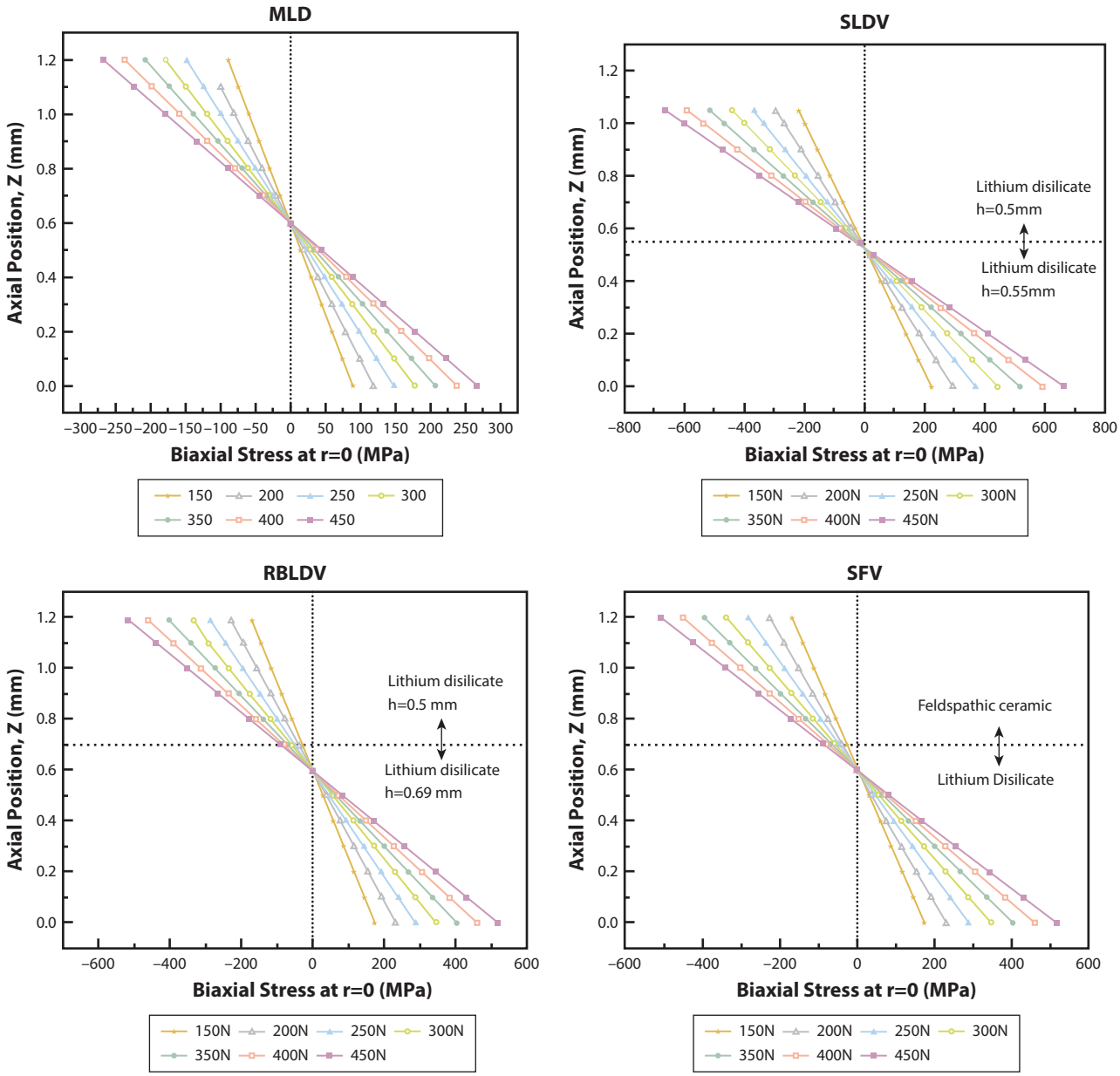

Figure 3. Stress distribution for each experimental group according to specimen thickness. MLD, monolithic lithium disilicate; RBLDV, resin-bonded lithium disilicate veneer; SLDV, sintered lithium disilicate veneer; SFV, sintered feldspathic veneer.

and sintered lithium disilicate veneer ($P<.05$) had significantly greater resistance to fracture than the sintered feldspathic veneer group. No statistically significant difference in resistance to fracture was observed between the sintered lithium disilicate veneer and resin-bonded lithium disilicate veneer groups compared with the monolithic lithium disilicate group. The difference between the monolithic lithium disilicate and sintered feldspathic veneer groups was not statistically significant ($P>.05$). The Weibull characteristic strength and Weibull modulus are presented in Table 2.

As seen in Figure 3, the BFS results for each group at the outer surface of each layer, Z=0 represents the bottom of the thicker lithium disilicate substructure, and the Z=1.2 or 1.05 represents the upper surfaces of the veneer layers. The positive stress values to the right of zero represent the tensile forces, while the negative stress values to the left of zero represent the compressive forces. Figure 4 shows the survival probability by using both a Kaplan-Meier and Weibull model for the various materials. Stress testing allowed determination of where the compressive and tensile forces were concentrated in the specimen at a certain load (Table 3).

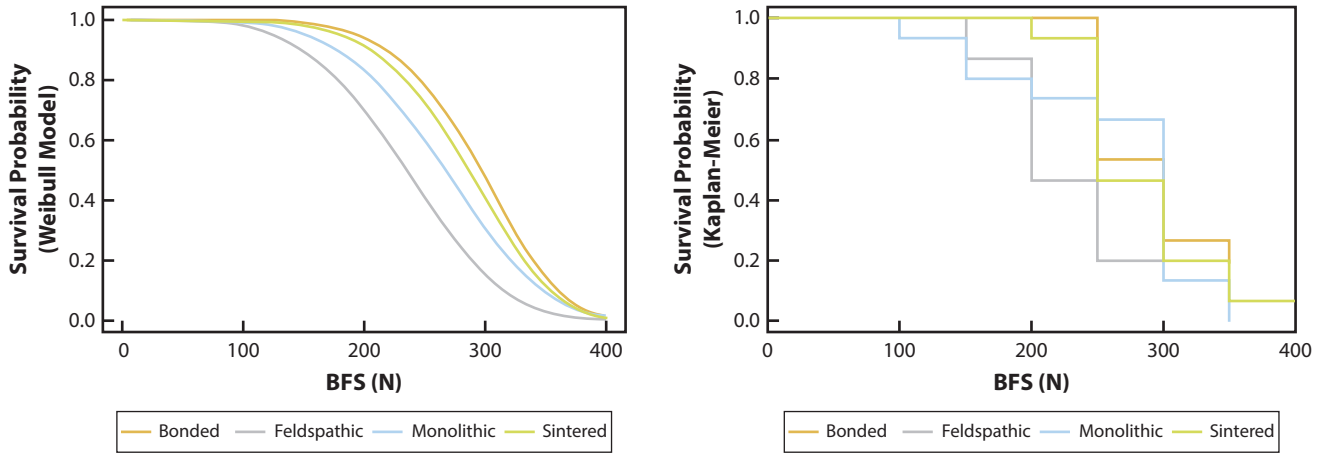

Figure 4. Survival graphs for stress until fracture. Data obtained by Weibull model and Kaplan-Meier. BFS, biaxial flexural stress.

Table 3. Biaxial flexural stress (MPa) on each layer of material at certain load (N)

	MLD	SLDV		RBLDV		SFV	
Load (N)	Tensile Stress LD1.2mm (MPa)	Tensile Stress LD0.55 (MPa)	Compressive Stress LD0.5mm (MPa)	Tensile Stress LD0.69 (MPa)	Compressive Stress LD0.5mm (MPa)	Tensile Stress LD0.70 (MPa)	Compressive Stress FP0.5mm (MPa)
150	169.43	221.32	221.50	172.31	172.45	172.57	169.13
200	225.90	295.10	295.34	229.75	229.93	230.09	225.51
250	282.38 (179.78*)	368.88 (182.55*)	369.17	287.19 (177.60*)	287.42	287.62 (182.78*)	281.89
300	338.86	442.65	443.01	344.63	344.90	345.14	338.27
350	395.34	516.43	516.84	402.06	402.39	402.66	394.64
400	451.81	590.21	590.68	459.50	459.87	460.19	451.02
450	508.29	663.98	664.51	516.94	517.35	517.71	507.40

FEA, finite element analysis; MLD, monolithic lithium disilicate; RBLDV, resin-bonded lithium disilicate veneer; SFV, sintered feldspathic veneer; SLDV, sintered lithium disilicate veneer.
*Maximum principal stress used as the failure criteria for the FEA at a load of 250 N (arbitrary load based on biaxial flexural stress test).

The number of resin-bonded lithium disilicate veneer fractured pieces (Table 2) was significantly greater than that in the other groups. In addition, the total number of cycles was analyzed by using a 1-way ANOVA with factor for group to identify the differences among the groups. The results were not statistically significant ($P>.05$ for monolithic lithium disilicate). As seen in Figure 5, which presents the SEM images that were qualitatively evaluated, the monolithic lithium disilicate specimen showed a uniform surface with no porosities or voids because of the homogenous characteristics observed in a manufactured lithium disilicate CAD material. The sintered lithium disilicate veneer group presented stress lines radiating from the sintered connecting porcelain at the base of the veneer specimen with occasional small voids within the material.

The sintered feldspathic veneer group showed a high number of porosities in the feldspathic porcelain. These imperfections can act to increase the stress within the feldspathic veneer, decreasing the material strength. The CAD materials were consistently more uniform, especially in comparison with the feldspathic material. As seen in Figure 6, the FEA results showed the MPS in each experimental group. At a load of 250 N (Table 3), arbitrary load based on the BFS test, the FEA showed that the group resin-bonded LD veneer presented lower MPS than groups monolithic lithium disilicate, sintered feldspathic veneer (182.78 MPa), and sintered lithium disilicate veneer. Figure 5 illustrates the maximum principal stress distribution (in MPa) at the surface of the bottom layer (where the tensile stresses were concentrated during the BFS test) for each experimental group. Group resin-bonded lithium disilicate veneer presented lower stress concentrations than the other groups.

DISCUSSION

The null hypothesis that adhering or sintering a thin veneer of lithium disilicate on another lithium disilicate surface would not result in increased fatigue resistance in comparison with feldspathic porcelain on lithium disilicate was rejected. Statistically significant differences were found between the sintered feldspathic veneer group and the groups with a sintered lithium disilicate veneer and with a resin-bonded lithium disilicate veneer in relation to the force the specimens could survive. The differences were probably because of differences in the

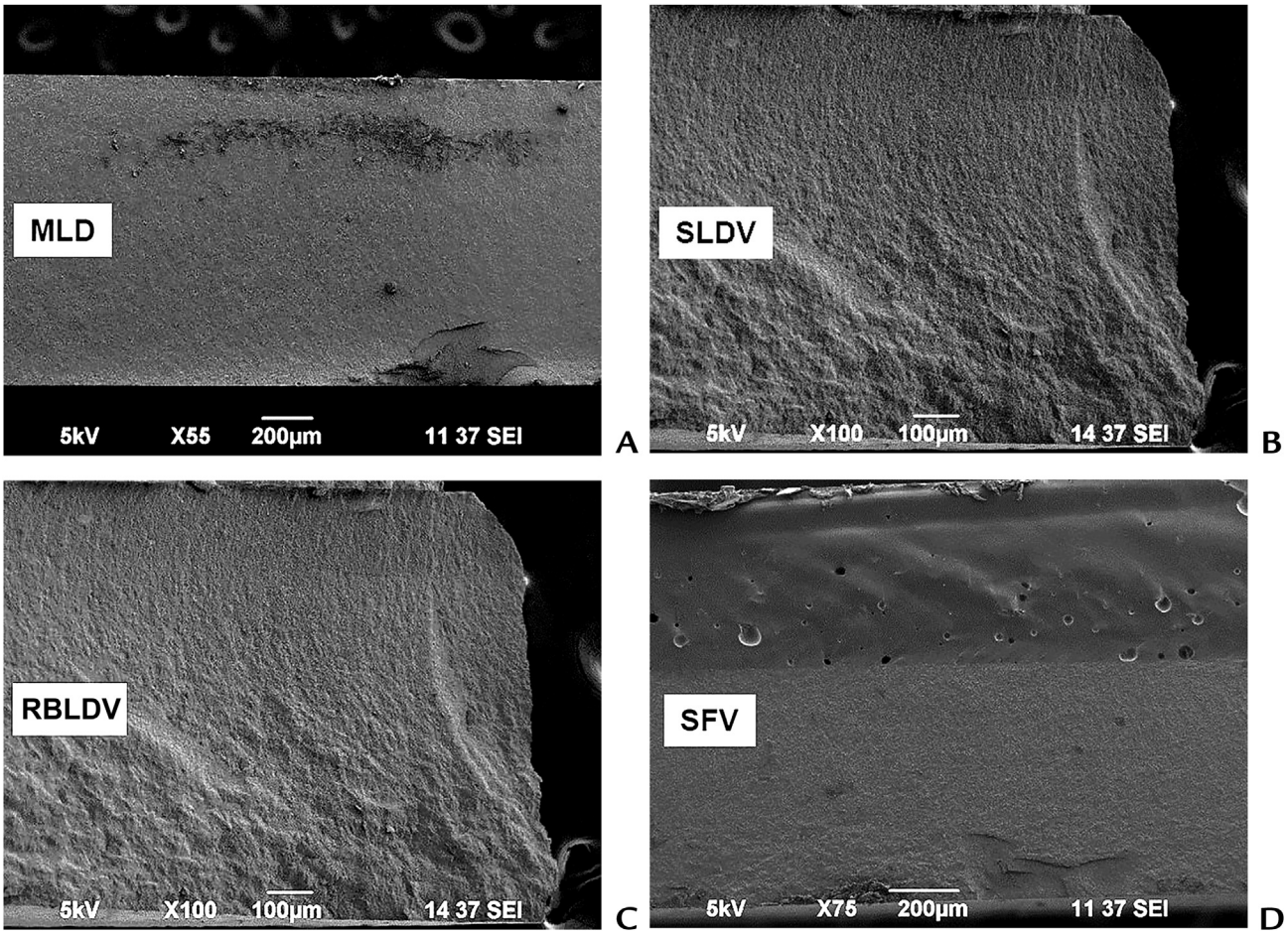

Figure 5. Scanning electron microscope images of specimens. A, Monolithic lithium disilicate (MLD). Original magnification ×55. B, Sintered lithium disilicate veneer. Original magnification ×100. C, Resin-bonded lithium disilicate veneer. Original magnification ×100. D, Sintered feldspathic veneer. Original magnification ×100. Note uniform density of all lithium disilicate specimens and contrasting voids seen throughout feldspathic porcelain on sintered feldspathic veneer and sintering layer of sintered lithium disilicate veneer. In addition, stress lines in sintered lithium disilicate veneer appear to originate at base of sintering layer and continue through lithium disilicate veneer above.

mechanical properties of the lithium disilicate and feldspathic porcelain.[1] However, the sintered feldspathic veneer group was not significantly different from the monolithic lithium disilicate group.

The cyclic stepwise fatigue test simulates occlusal contacts, leading to slow crack growth starting at a critical defect.[16] The Weibull analysis characterizes the fracture potential of ceramic materials,[17] and the Weibull modulus (m) shows the variation in strength distribution resultant from the presence of flaws in the microstructure.[18] A lower Weibull modulus indicates the presence of a greater number of flaws, and a higher Weibull modulus indicates superior structural integrity.[18,19] In the present study, the groups with sintered lithium disilicate veneer and resin-bonded lithium disilicate veneer presented a lower probability of failure and higher strength than sintered feldspathic veneer. The results can be explained by the presence of pores on the veneering surface of the feldspathic porcelain.

When evaluating the stress distribution in the specimens (150 N to 450 N), the monolithic lithium disilicate and sintered lithium disilicate veneer groups had similar compressive and tensile stresses. The resin-bonded lithium disilicate veneer group presented compressive forces on the 0.5-mm veneering lithium disilicate layer and approximately 1 mm below the neutral axis. For the sintered feldspathic veneer, all the compressive stress was concentrated in the feldspathic porcelain, a ceramic with low flexural strength.[20] Therefore, the use of feldspathic veneer could explain this group's inferior performance after the fatigue cycle. In addition, feldspathic porcelain contains increased glassy phase and reduced mechanical properties compared with lithium disilicate ceramic. The stress distribution and failure are materially related, showing that for bilayers, lithium disilicate sintered to lithium disilicate with connecting porcelain or the lithium disilicate resin-bonded to lithium disilicate is recommended. For the sintered lithium disilicate veneer

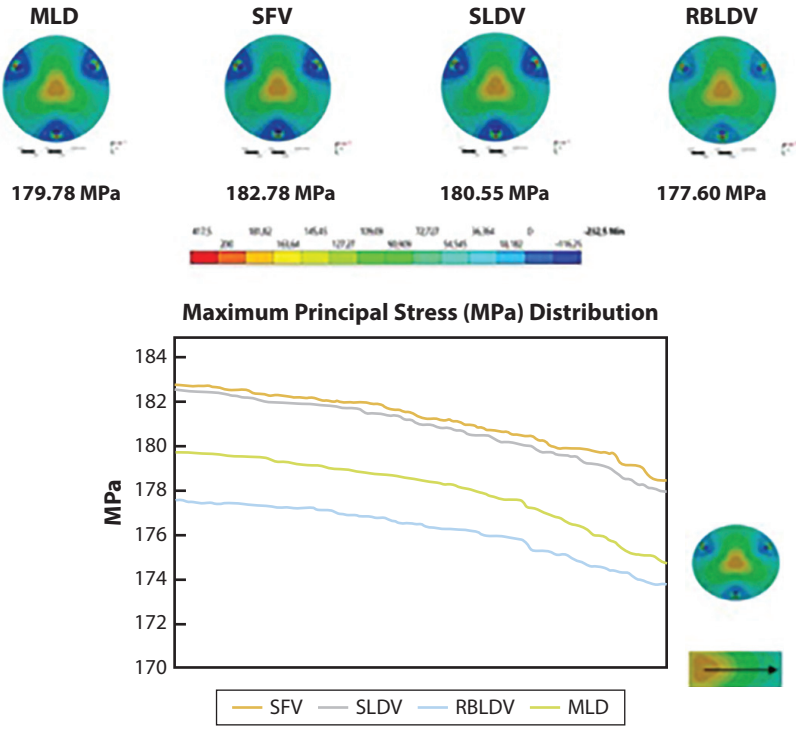

Figure 6. Maximum principal stress (MPa) of each group at tension surface and MPS distribution at surface of bottom layer of each group from center to edge. MLD, monolithic lithium disilicate; RBLDV, resin-bonded lithium disilicate veneer; SLDV, sintered lithium disilicate veneer; SFV, sintered feldspathic veneer.

group, it was necessary to reduce the size of the substructure disk because of the 0.15-mm thickness of the connecting porcelain to maintain a minimum 0.8-mm thickness of the core lithium disilicate veneer as recommended by the manufacturer.[7] The reduction in thickness from 0.7 mm to an average of 0.55 mm may have led to a reduced resistance to fracture for those specimens. FEA showed that the reduction in the thickness of the core structure by half would double the percentage of fracture for that specimen.[21] The core and veneer ratio of 0.7 had a significant decrease in strength, but there was little gain beyond the 1:1 ratio.

The present study used a single-bottle etchant and primer to bond lithium disilicate to lithium disilicate structures rather than the hydrofluoric acid etch and a silane coupling agent.[22,23] The use of ammonium polyfluoride and trimethoxypropyl mechacrylate for silanization in a single bottle application was designed to etch the surface while depositing a layer of silane in a single step. No statistically significant bond strength differences between the 2 techniques have been reported,[22] attributed to the strong bond that can form between the silica in the ceramic and fluoride with ammonium polyfluoride.[22]

From the FEA analysis, the resin-bonded lithium disilicate veneer group presented lower MPS values than all other groups, indicating higher resistance to fracture. The resin interface may have helped to distribute stresses better than the other groups. However, the FEA model considers a flawless structure, and the specimens from groups sintered feldspathic veneer, sintered lithium disilicate veneer, and monolithic lithium disilicate presented similar behavior, different from the mechanical test. The BFS test showed that sintered feldspathic veneer presented lower mechanical resistance than resin-bonded lithium disilicate veneer and sintered LD veneer, with no statistically significant difference from monolithic lithium disilicate. This can be explained by the presence of flaws and porosities in the feldspathic porcelain, confirmed by SEM analysis. Therefore, FEA is an important tool for predicting the stress distribution in perfect materials and helps in the design of new materials; however, limitations are applied considering the fabrication method used. Although this introductory study seems to indicate that a lithium disilicate CAD-CAM–fabricated veneer is comparable with monolithic lithium disilicate and that it may be stronger than a feldspathic porcelain hand-fabricated veneer, additional studies are recommended before routine clinical application.

CONCLUSIONS

Based on the findings of this in vitro study, the following conclusion was drawn:

1. Laminating the lithium disilicate substructure with a lithium disilicate veneer (resin-bonded or sintered)

could produce specimens with a fracture resistance similar to that of a monolithic restoration of the same dimensions.

REFERENCES

1. Porto TS, Roperto RC, Akkus A, Akkus O, Teich S, Faddoul F, et al. Effect of storage and aging conditions on the flexural strength and flexural modulus of CAD/CAM materials. Dent Mater J 2019;38:264-70.
2. Guess PC, Schultheis S, Bonfante EA, Coelho PG, Ferencz JL, Silva NR. All-ceramic systems: laboratory and clinical performance. Dent Clin North Am 2011;55:333-52. ix.
3. Willard A, Gabriel Chu TM. The science and application of IPS e.Max dental ceramic. Kaohsiung J Med Sci 2018;34:238-42.
4. Hooshmand T, Parvizi S, Keshvad A. Effect of surface acid etching on the biaxial flexural strength of two hot-pressed glass ceramics. J Prosthodont 2008;17:415-9.
5. Zogheib LV, Bona AD, Kimpara ET, McCabe JF. Effect of hydrofluoric acid etching duration on the roughness and flexural strength of a lithium disilicate-based glass ceramic. Braz Dent J 2011;22:45-50.
6. Fasbinder DJ, Dennison JB, Heys D, Neiva G. A clinical evaluation of chairside lithium disilicate CAD/CAM crowns: a two-year report. J Am Dent Assoc 2010;141(Suppl 2):10S-4S.
7. Zaher AM, Hochstedler JL, Rueggeberg FA, Kee EL. Shear bond strength of zirconia-based ceramics veneered with 2 different techniques. J Prosthet Dent 2017;118:221-7.
8. Albakry M, Guazzato M, Swain MV. Biaxial flexural strength, elastic moduli, and x-ray diffraction characterization of three pressable all-ceramic materials. J Prosthet Dent 2003;89:374-80.
9. Wagner WC, Chu TM. Biaxial flexural strength and indentation fracture toughness of three new dental core ceramics. J Prosthet Dent 1996;76:140-4.
10. Lin WS, Ercoli C, Feng C, Morton D. The effect of core material, veneering porcelain, and fabrication technique on the biaxial flexural strength and weibull analysis of selected dental ceramics. J Prosthodont 2012;21:353-62.
11. International Organization for Standardization. ISO 6872. Dentistry - Ceramics. Geneva: International Organization for Standardization; 2015.
12. Anami LC, Lima JM, Valandro LF, Kleverlaan CJ, Feilzer AJ, Bottino MA. Fatigue resistance of Y-TZP/porcelain crowns is not influenced by the conditioning of the intaglio surface. Oper Dent 2016;41:E1-12.
13. Schmitter M, Schweiger M, Mueller D, Rues S. Effect on in vitro fracture resistance of the technique used to attach lithium disilicate ceramic veneer to zirconia frameworks. Dent Mater 2014;30:122-30.
14. Sawada T, Schille C, Wagner V, Spintzyk S, Schweizer E, Geis-Gerstorfer J. Biaxial flexural strength of the bilayered disk composed of ceria-stabilized zirconia/alumina nanocomposite (Ce-TZP/A) and veneering porcelain. Dent Mater 2018;34:1199-210.
15. Hsueh CH, Luttrell CR, Becher PF. Analyses of multilayered dental ceramics subjected to biaxial flexure tests. Dent Mater 2006;22:460-9.
16. Madruga CFL, Bueno MG, Dal Piva AMO, Prochnow C, Pereira GKR, Bottino MA, et al. Sequential usage of diamond bur for CAD/CAM milling: Effect on the roughness, topography and fatigue strength of lithium disilicate glass ceramic. J Mech Behav Biomed Mater 2019;91:326-34.
17. Tinschert J, Zwez D, Marx R, Anusavice KJ. Structural reliability of alumina-, feldspar-, leucite-, mica- and zirconia-based ceramics. J Dent 2000;28:529-35.
18. Elsaka SE, Elnaghy AM. Mechanical properties of zirconia reinforced lithium silicate glass-ceramic. Dent Mater 2016;32:908-14.
19. Bona AD, Anusavice KJ, DeHoff PH. Weibull analysis and flexural strength of hot-pressed core and veneered ceramic structures. Dent Mater 2003;19:662-9.
20. Thompson VP, Rekow DE. Dental ceramics and the molar crown testing ground. J Appl Oral Sci 2004;12:26-36.
21. Anusavice KJ, Jadaan OM, Esquivel-Upshaw JF. Time-dependent fracture probability of bilayer, lithium-disilicate-based, glass-ceramic, molar crowns as a function of core/veneer thickness ratio and load orientation. Dent Mater 2013;29:1132-8.
22. Al-Harthi AA, Aljoudi MH, Almaliki MN, El-Banna KA. Laboratory study of micro-shear bond strength of two resin cements to leucite ceramics using different ceramic primers. J Contemp Dent Pract 2018;19:918-24.
23. Alrahlah A, Awad MM, Vohra F, Al-Mudahi A, Al Jeaidi ZA, Elsharawy M. Effect of self etching ceramic primer and universal adhesive on bond strength of lithium disilicate ceramic. J Adhes Sci Technol 2017;31:2611-9.

Corresponding author:
Dr Sabrina Feitosa
Indiana University School of Dentistry
1121 W Michigan Street
Indianapolis, IN 46202
Email: sfeitosa@iu.edu

Acknowledgments
This article was based on a master's thesis project done by the primary author, Jaren T. May, with the title "Stepwise stress testing of different CAD/CAM lithium-disilicate veneer application methods to lithium-disilicate substructure" at Indianan University School of Dentistry.
The authors thank Mr George Eckert, Department of Biostatistics, Indiana University School of Medicine, and Richard M. Fairbanks, School of Public Health, for conducting the statistical analyses. The authors would like to thank Ms Caroline Miller, Indiana University School of Medicine Electron Microscopy Center, for performing the scanning electron microscope imaging.
The views expressed in this article reflect those of the primary author and do not necessarily reflect the official policy or position of the Department of the Navy, Department of Defense, nor the United States Government.
The primary author states: "I am a military service member of the United States government. This work was prepared as part of my official duties. Title 17 USC 105 provides that copyright protection under this title is not available for any work of the United States Government."
Title 17 USC 101 defines a US Government work as work prepared by a military service member or employee of the US Government as part of that person's official duties.

CRediT authorship contribution statement
Jaren T. May: Conceptualization, Methodology, Investigation, Formal analysis, Writing - original draft. **Anelyse Arata:** Methodology, Writing - original draft, Formal analysis. **Norman B. Cook:** Methodology, Writing - original draft. **Kim E. Diefenderfer:** Methodology, Writing - original draft. **Nelson B. Lima:** Formal analysis, Writing - original draft. **Alexandre L.S. Borges:** Methodology, Investigation, Writing - original draft. **Sabrina Feitosa:** Conceptualization, Methodology, Writing - original draft, Formal analysis.

https://doi.org/10.1016/j.prosdent.2020.05.033